IDENTIFICATION OF COUPLED DYNAMICS IN PLATE BY PROCESSING THE FREE DYNAMICS USING THE PROPER ORTHOGONAL DECOMPOSITION

[1]MOHAMMAD BANI-KHALED, [2]HAMZA SH. AL-SERHAN

[1] Assistant professor, Applied Science Private University, Amman, Jordan
E-mail: [1]m_banikhaled@asu.edu.jo

Abstract— Mechanical structures are composed of combinations of different structural elements, such as beams, rods, flexible plates, disks etc. The nonlinear behavior of shells and plates is one of the challenges that the researches need to face. The FE methods are highly involved in the analysis of generic shells. They are effective in analyzing arbitrary geometries composed of linear, composite, or nonlinear materials. However, FE produces the discrete dynamics in the form of numerical databases that some information are hidden in. Based on that it is necessary to develop methodologies capable to process the FE discrete results and obtain -if possible- the structure properties.
Here the POD transform will be applied to process the discrete dynamics of plate structures. Using the POD transform, numerical simulations of free motions of rectangular plates will be viewed in terms of POD modes. It will be examined whether the POD modes have any relations with the Normal modes of vibration (natural frequencies and shapes).

Keywords— Shells and Plates, Coupled Dynamics, Nonlinear Dynamics, Proper Orthogonal Decomposition.

I. INTRODUCTION

Thin plate structures are extensively used in modern engineering application. And usually they are subjected to severe dynamic loading (airplanes, ships, pressure vessels, rocket etc.). Due to their operation conditions, large amplitude vibrations are always expected to take place. If the vibration amplitudes are of the same order of the thickness of the plate, a significant geometrical nonlinearity will exist [12, 13]. This will lead to a change in the dynamic properties (natural frequencies and mode shapes) of the system.

The most widely used nonlinear equations of motion for thin plates are the von Karman dynamic equations of motion [13]. Due to the complexity of these coupled nonlinear partial differential equations there is no exact solution known yet. Hence, each problem has received a special treatment involving some particular approximations.

Most of the studies that carried out on large amplitudes vibration of plates are done by assuming space modes or time functions. In the assumed space modes method, spatial functions that satisfy the related boundary conditions (usually the linear mode shapes) combined with Galerkin methods are used to eliminate the space variable from the governing equations. The problem is then reduced, in the case of single-mode approach, to the well-known Duffing equation in time. This equation may be solved in terms of elliptic functions [14], harmonic balance method [9] or the perturbation methods [4, 5].

A multiple-mode approach (three modes) has been presented in [13], in which the steady-state axisymmetric free and forced response of clamped circular plates has been investigated by using the Galerkin procedure and the harmonic balance method. Recently, the geometrically nonlinear free axisymmetric vibrations of clamped circular plates have been studied by using a multimode model, taking into account the coupling between the higher vibration modes [7]. The main feature of this multimodal model, which is based on Hamilton's principle and spectral analysis, is that it makes the geometrically nonlinear effects appear, not only via the amplitude frequency dependence, which was the main purpose of most studies on nonlinear vibrations, but also via the dependence of the structure deflection shapes on the amplitude of vibration. This allows quantitative estimates of nonlinear stresses to be obtained in sensitive regions of the structure, which may be of crucial importance in the fatigue life prediction of structures working in or exposed to a severe environment.

In the assumed time function method, a simple harmonic function in time is assumed and is then eliminated from the equation of motion using the Kantorovich averaging procedure [8]. The resulting nonlinear spatial boundary value problem is solved numerically.

Some other studies are based on a simplified nonlinear equation, obtained using Berger's hypothesis [1]. Also, different perturbation techniques were used in the study of nonlinear vibrations of circular plates [10, 11]. Another work was based on the invariant manifold approach, by showing the existence of a global nonlinear invariant manifold in the phase space. The invariant manifold carries a continuum of slow periodic motion [4].

The finite element method was first used to investigate the large displacement by Turner 1960, but the first application of large displacement analysis of thin plates and shells was done by Gallagher. Maecal used the nonlinear displacement strain relationship from the classical theory of elasticity and demonstrated that the initial stress and the initial displacements matrices are of the same order, since then, in the last two decades significant progress in developing reliable computational algorithms for nonlinear FE method. Remarkable work in the field of FE method for plates was done by Clough and Tocher, Argyn Zienkiewich ,Bathe [1995] and many others.

2. KINEMATICS AND EQUATION OF MOTION

Consider a Cartesian coordinate system (x, y, z), and let (x, y) be the in-plane coordinate of a point at the middle surface of the plate, and z is the transverse coordinate, Fig.1.

Let $\{u, v, w\}$ denote the Cartesian components of the displacement vector of a point on the plate in the x, y, and z directions respectively. The displacements are approximated as follows:

$$u(x,y,z) = u_0(x,y) - z\phi_x \frac{\partial w_0}{\partial x},$$
$$v(x,y,z) = v_0(x,y) - z\phi_y \frac{\partial w_0}{\partial y}, \qquad (1)$$
$$w(x,y,z) = w_0(x,y),$$

where $\{\phi_x, \phi_y\}$ are the rotations of the transverse normal about the y and z axes respectively, and $\{u_0(x,y), v_0(x,y), w_0(x,y)\}$ denote the components of the displacements vector of a point on the plane z=0, the so called neutral plane. For thin plates (the in plane characteristic dimension to the thickness is in the order of 50 or greater) the rotation functions are approximated to be equal to slopes of the transverse deflection:

$$\phi_x = -\frac{\partial w_0}{\partial x}, \phi_y = -\frac{\partial w_0}{\partial y} \qquad (2)$$

The Von-Karman nonlinear strains associated with the displacement fields are expressed as given in (4) and the equations of motion are derived from the principle of virtual work.

$$\delta W_e \equiv \delta U_e + \delta V_e = 0. \qquad (3)$$

The coupled nonlinear partial differential equations of motion (Von-Karman plate theory) are given in equations (6). In these equations we can see that the dynamics evolve nonlinear coupling between the three displacement fields of the middle surface. The Von-Karman model is a nonlinear model with limited predictability since it cannot predict independently the rotations of material lines perpendicular to the middle surface. The rotations are directly related to the partial derivatives of the transverse displacement.

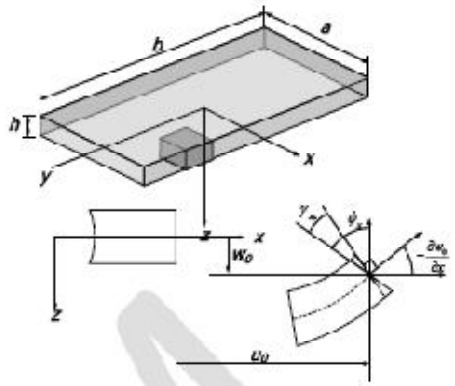


Fig.1. Plate kinematics

$$\begin{Bmatrix} \varepsilon_{xx} \\ \varepsilon_{yy} \\ \gamma_{yz} \\ \gamma_{xz} \\ \gamma_{xy} \end{Bmatrix} = \begin{Bmatrix} \frac{\partial u_0}{\partial x} + \frac{1}{2}\left(\frac{\partial w_0}{\partial x}\right)^2 \\ \frac{\partial v_0}{\partial y} + \frac{1}{2}\left(\frac{\partial w_0}{\partial y}\right)^2 \\ \frac{\partial w_0}{\partial y} + \phi_y \\ \frac{\partial w_0}{\partial x} + \phi_x \\ \frac{\partial u_0}{\partial y} + \frac{\partial v_0}{\partial x} + \frac{\partial w_0}{\partial x}\frac{\partial w_0}{\partial y} \end{Bmatrix} + z \begin{Bmatrix} \frac{\partial \phi_x}{\partial x} \\ \frac{\partial \phi_y}{\partial y} \\ 0 \\ 0 \\ \frac{\partial \phi_x}{\partial y} + \frac{\partial \phi_y}{\partial x} \end{Bmatrix}. \qquad (4)$$

It is not yet known whether a closed form solution for these nonlinear equations is possible to obtain. However, closed from solutions are possible for the linearized equations defined on simple domains. The solution procedure for the linearized equations is to search for elementary modal motions by assuming solutions products in time and space:

$$u(x,y,z,t) - U(x,y)e^{i\omega t}$$
$$v(x,y,z,t) - V(x,y)e^{i\omega t} \qquad (5)$$
$$w(x,y,z,t) - W(x,y)e^{i\omega t}$$

and applying appropriate boundary conditions. For example, for the simply supported rectangular plate the boundary conditions are:

$$w = w_{xx} = u = 0, \quad \text{at } x = 0, a$$
$$w = w_{yy} = v = 0, \quad \text{at } y = 0, b$$

As we have mentioned before, linearization means the highest degree of simplification in regard to the nonlinearity of the problem. Implications, especially linearization, lower the predictability of the simplified model.

The method of Finite Elements can be used to derive computational models for the nonlinear coupled partial differential equations of motion of a

plate. The simulated dynamics will be analyzed in terms of Proper Orthogonal modes. The POD-based methodology allows us to analyze high fidelity mathematical models for plates by taking full advantage of accurate numerical simulations. The challenging issue here is how to use the Discrete Time-POD transform for one-dimensional multi-field dynamics to analyze the multi-field dynamical processes defined over two-dimensional domains.

$$\frac{\partial^2 u}{\partial x^2}+\frac{\partial w}{\partial x}\frac{\partial^2 w}{\partial x^2}+\frac{(1+\nu)}{2}\left(\frac{a}{b}\frac{\partial^2 \upsilon}{\partial x\partial y}+\frac{a^2}{b^2}\frac{\partial w}{\partial y}\frac{\partial^2 w}{\partial x\partial y}\right)+\frac{(1-\nu)}{2}\left(\frac{a^2}{b^2}\frac{\partial^2 u}{\partial y^2}+\frac{a^2}{b^2}\frac{\partial w}{\partial x}\frac{\partial^2 w}{\partial y^2}\right)=\frac{\varepsilon}{12}\ddot{u},$$

$$\frac{\partial^2 \upsilon}{\partial y^2}+\frac{a}{b}\frac{\partial w}{\partial y}\frac{\partial^2 w}{\partial y^2}+\frac{(1+\nu)}{2}\left(\frac{b}{a}\frac{\partial^2 u}{\partial x\partial y}+\frac{b}{a}\frac{\partial w}{\partial x}\frac{\partial^2 w}{\partial x\partial y}\right)+\frac{(1-\nu)}{2}\left(\frac{b^2}{a^2}\frac{\partial^2 \upsilon}{\partial x^2}+\frac{b}{a}\frac{\partial w}{\partial y}\frac{\partial^2 w}{\partial x^2}\right)=\frac{\varepsilon}{12}\frac{b^2}{a^2}\ddot{\upsilon},$$

$$\frac{\partial^4 w}{\partial y^4}+2k\frac{\partial^4 w}{\partial x^2\partial y^2}+k^2\frac{\partial^4 w}{\partial y^4}+\frac{\partial^2 w}{\partial t'^2}+\varepsilon\left\{\begin{array}{l}2c\dfrac{\partial w}{\partial t'}+k\gamma\dfrac{\partial^4 w}{\partial x^2\partial y^2}+k\gamma\dfrac{\partial^4 w}{\partial y^4}-12\dfrac{\partial u}{\partial x}\dfrac{\partial^2 w}{\partial x^2}-\\ 6\left(\dfrac{\partial w}{\partial x}\right)^2\dfrac{\partial^2 w}{\partial x^2}-\\ 12\nu\left(\dfrac{a}{b}\dfrac{\partial \upsilon}{\partial y}\dfrac{\partial^2 w}{\partial x^2}+\dfrac{1}{2}k\left(\dfrac{\partial w}{\partial y}\right)^2\dfrac{\partial^2 w}{\partial x^2}\right)\\ -12\dfrac{a}{b}k\dfrac{\partial \upsilon}{\partial y}\dfrac{\partial^2 w}{\partial y^2}-6k^2\left(\dfrac{\partial w}{\partial y}\right)^2\dfrac{\partial^2 w}{\partial y^2}-\\ 12\nu\left(k\dfrac{\partial u}{\partial x}\dfrac{\partial^2 w}{\partial y^2}+\dfrac{1}{2}k\left(\dfrac{\partial w}{\partial x}\right)^2\dfrac{\partial^2 w}{\partial y^2}\right)-12(1-\nu)\\ \left(k\dfrac{\partial u}{\partial y}\dfrac{\partial^2 u_3}{\partial x\partial y}+\dfrac{a}{b}\dfrac{\partial \upsilon}{\partial x}\dfrac{\partial^2 u_3}{\partial x\partial y}+k\dfrac{\partial u_3}{\partial x}\dfrac{\partial u_3}{\partial y}\dfrac{\partial^2 u_3}{\partial x\partial y}\right)\end{array}\right.=\varepsilon F(x,y,t)+O(\varepsilon^2) \quad (6)$$

3. POD Analysis of Free Linear Vibrations

In the FE-based discrete models, shell elements are used to model structures in which the thickness is significantly smaller than the other dimensions. Conventional shell elements are used to discretize a body by defining the geometry at a reference surface. Conventional shell elements have displacement and rotational degrees of freedom. In our case we selected a shell element in which the transverse shear calculation is performed at the center of the element and assumed constant thought the thickness of the element. The time integration of the FE model used is based on the Total Lagrangian formulation, in which all the displacements and rotations are related to the initial configuration of the plate. A four-node shell element is used. Each node has six DOF: the first three denote displacements and the other three denote independent rotations of the material lines normal to the middle-surface

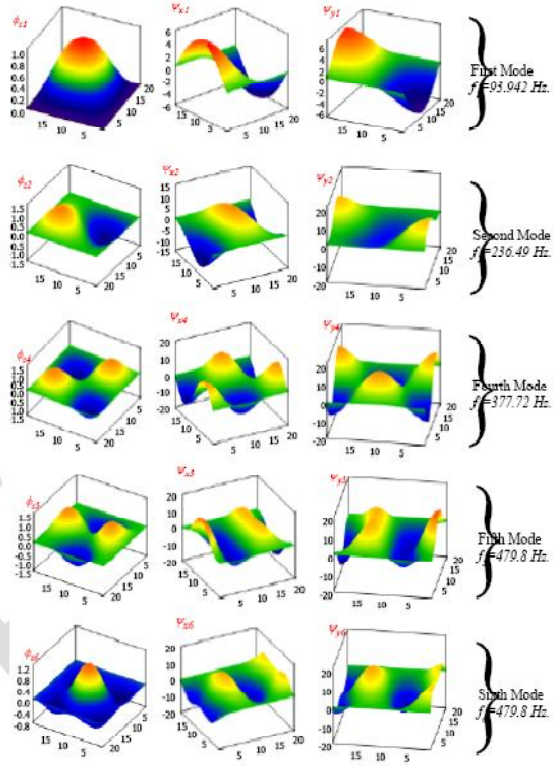


Fig.2.: The first 5 normal modes of vibrations obtained using the FE method

In the discrete POD, the dynamics of a motion of the plate is described mathematically by the following vector-valued field:

$$\boldsymbol{U}(x,y,t)=\left\{\begin{array}{l}U_1(x,y,t)\\ U_2(x,y,t)\\ U_3(x,y,t)\\ R_1(x,y,t)\\ R_2(x,y,t)\\ R_3(x,y,t)\end{array}\right\} \quad (7)$$

The fields $U_1(x,y,t), U_2(x,y,t), U_3(x,y,t)$ represent the three components of the displacement vector which is coupled to the three fields $R_1(x,y,t)$, $R_2(x,y,t)$, $R_3(x,y,t)$ representing the rotation vector. The six fields are distributed over the middle-surface.

In this work , we want to analyze the dynamics for the linear rectangular plate. In particular, the properties of the coupled dynamics as viewed in terms of POD modes extracted from the free vibration analysis of the plate will be compared with the properties of the normal modes of vibration.

The plate that we wish to analyze is simply supported along the edges. In order to excite many modes of vibrations, the plate is exposed to an impact load at its center. The modes with high frequencies will decay faster due to the damping, while the low modes of vibrations will have a longer duration.

The simulated dynamics are analyzed by a novel use of the Discrete Time-POD transform for one-dimensional multi-field dynamics. In particular, the two-dimensional snapshots forming the discrete dynamics of a motion of the plate are properly vectorized and thus the new one-dimensional snapshot matrix, equivalent to the original one, can be processed by the Discrete Time-POD transform for one-dimensional multi-field dynamics [4-6].

4. The POD Transform Results

The POD transform shows that the free dynamics of the motion of the plate caused by the central impulsive force is represented by a small number of POD modes. The first six POD modes contain more than 99.9% of the total auto-correlation energy of the motion. Recall that by definition the autocorrelation energy is identified with the trace of the time auto-correlation matrix [5].

Table.1: The normalized energy fractions, of each POD mode.

m	λm	$\Sigma\lambda m$
1	0.9425111	0.9425111
2	0.0483642	0.9908753
3	0.0042681	0.9951434
4	0.0024425	0.9975858
5	0.0011371	0.9987230
6	0.0006162	0.9993392
7	0.0003299	0.9996691
8	0.0001440	0.9998132
9	0.0000801	0.9998932

4.1 The First POD Mode

The first POD mode contains about 94.25 % of the total autocorrelation energy. According to the POD procedure, the first mode is written as a product of three elements:

$$\boldsymbol{U}_1(x,y,t) = \sqrt{\lambda_1}\boldsymbol{A}_1(t)\boldsymbol{\Phi}_1(x,y), \qquad (8)$$

where element $\sqrt{\lambda_1}$, equal to 0.9708, is the modal participation factor, elements $\boldsymbol{A}_1(t)$ is the modal amplitude, and element $\boldsymbol{\Phi}_1(x,y)$ is the modal shape. Fig.3 is a plot for the discrete amplitude of the first POD mode. It represents a harmonic motion with a single frequency equal to 97.6 Hz. This frequency is close to the first natural frequency of the simply supported plate.

The other element of the first POD mode is the shape function $\boldsymbol{\Phi}_1(x,y)$. The mode shape is composed of three components $\{\varphi_{31}(x,y), \psi_{11}(x,y), \psi_{21}(x,y)\}$: the deflection in the z direction and the two bending-shearing components about the x and y axes. The first component, Fig.4A, is the deflection mode in the z direction, while the other two components are the shearing-bending modes of the plate in the x-direction and y-direction. We can see that those modes are similar to that we obtained from the eigenvalue analysis. The result is important since we extracted the coupled mode shape for the simply supported rectangular plate from the dynamic database that obtained from numerical FE solution.

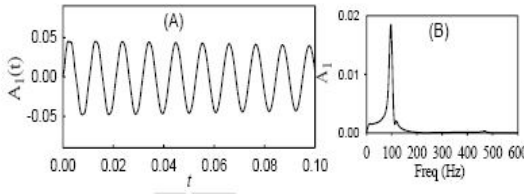


Fig.3: The amplitude of the first POD mode (A) and its FFT (B).

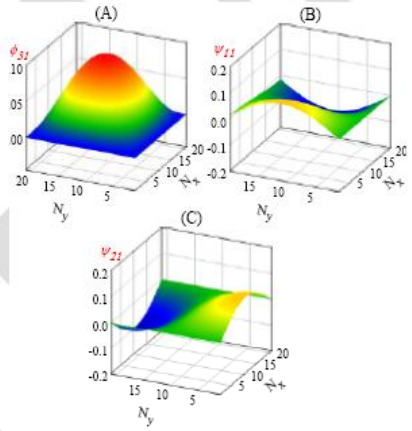


Fig.4:The mode shapes for the first POD mode: (A) displacement (B) rotation about the x-axis and (c) is the rotation about the y-axis.

In order to study the coupling during this mode, the norms of the POD mode shape components will give direct information. In Fig.5, we can see that the dominant motions are the bending-shearing with almost equal strength, while the translation of the plate in the z direction contains less energy. In order to compare the shapes of the POD modes with the shapes of the linear normal modes we use the L2 norms. Fig.5 reveals that the norms of the components of the first POD mode are nearly equal to those of a linear normal mode.

Summarizing the first POD mode, it is dominant with more than 94% of the total energy. The single frequency in its amplitude is almost equal to the natural frequency of the same plate. And the components of its shape are similar to those of a normal mode. These similarities between the POD results and the eigenvalue results give evidence that this POD mode represents a normal mode of vibration.

4.2 The Second POD Mode

The second POD mode contains 4.82% of the total energy. The amplitude of this POD mode has a

single frequency equal to 468.5 Hz, Fig.6. This frequency is approximately equal to the frequency of the fifth normal mode of vibration of the plate. The reason for which we see the fifth mode is due to the location of the applied impact force (at the middle of plate): the symmetric modes that have maximum deflection at the center of the plate will be excited.

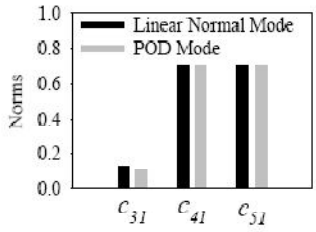


Fig.5: The norms of the first POD mode shape components (gray) compared to that of the linear mode shape (black).

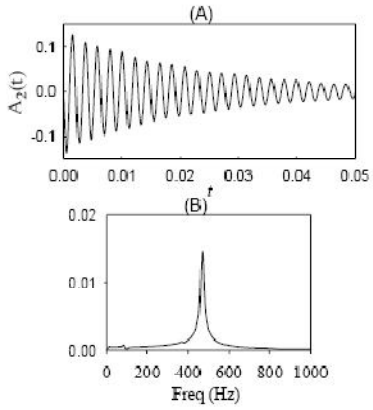


Fig.6: The second POD mode: (A) Amplitude, and (B) the FFT analysis.

The second POD mode shape can is expressed as:

$$U_2(x,y,t) = \sqrt{\lambda_2} A_2(t) \Phi_2(x,y) \qquad (9)$$

where the $A_2(t)$ is the amplitude plotted in Fig.6, and the $\Phi_2(x,y)$ is the mode shape, which composed of $\{\varphi_{32}(x,y), \psi_{12}(x,y), \psi_{22}(x,y)\}$. Plots for these components are shown in Fig.7.

It seems that the shape of the second POD mode is similar to that of the sixth linear normal mode. In this mode, a strong coupling exists between the two bending-shearing components, while displacement mode has a relatively small share in the mode. Also, from the comparison between the norms of the mode shapes components that are extracted using the POD transform, and the normal mode we can see that they are identical. This gives evidence that the second POD mode is also a normal mode of vibration.

5 The Third, Fourth and Fifth POD Modes

The next three POD modes have normalized energy fractions equal to $\{0.0042, 0.00244, 0.00113\}$ respectively. The energy content in these modes is small compared to the first and second modes. But they are important because they are related to the early stage of the dynamic excitation of the plate (fast vibrations and waves). The impact excited many high and low modes of vibration, bending and shearing coupled together. But the modes with relatively high frequencies decays fast due to the system damping. The interesting fact is if they represent linear normal modes with very small action (small energy), they are captured in a Proper Orthogonal Decomposition of a database. The amplitudes of the third, fourth and fifth POD modes are shown in Fig.9. We can notice from their time distribution that they are related to the early stage of the dynamics. The amplitudes are harmonic vibrations each with a single frequency. The frequencies are almost identical to the natural frequencies of the simply supported rectangular plate. The frequencies and their corresponding natural frequencies are summarized in Table-2.

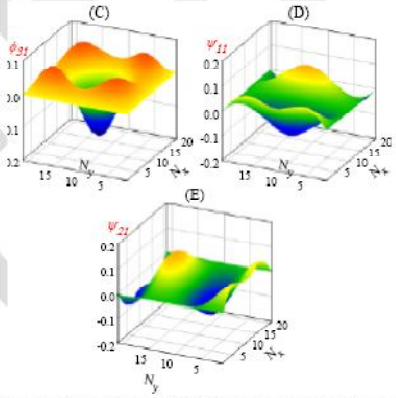


Fig.7: The shapes of the second POD mode, (A) displacement, (B) shearing mode about x-direction, (c) shearing in y-direction.

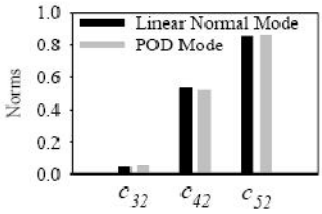


Fig.8: The norms of the second POD mode shape components (gray) compared to that of the linear mode shape (black).

Plots for the third, fourth and fifth POD mode shapes are present in Fig.10.

The important benefit we got from the previous analysis is that we can rewrite the dynamics of the plate using the reduced system dynamics that we obtain from the POD transform analysis. The dynamics can be represented by a finite number of optimal modes:

$$U(x,y,t) \cong \sum_{m=1}^{M} \sqrt{\lambda_m} A_m(t) \Phi_m(x,y) \qquad (10)$$

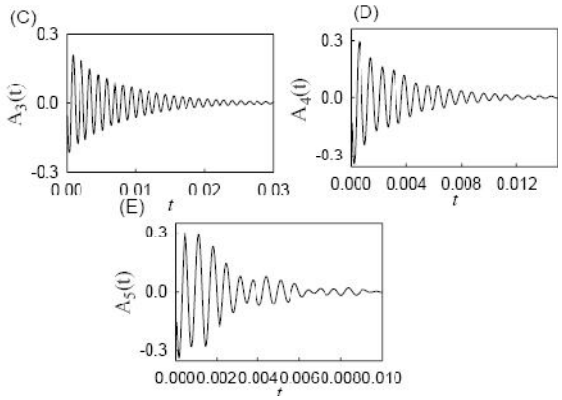


Fig.9: The amplitudes of the third (A), the fourth (B) and the fifth (C) POD modes.

Table.2: The single frequencies of the POD modes versus linear natural frequencies.

m	Energy	POD Ampl. Freq	Linear Natural Freq.
1	0.9073287	97.6074	93.942
2	0.0324921	370.9081	377.72
3	0.0502108	468.5155	479.80
4	0.0040299	819.9022	832.65
5	0.0023368	1220.093	1203.01

From the analysis of the coupled linear dynamics using the POD transform, we managed to extract the natural frequencies and the normal modes of vibration from the POD modes. These results were expected, since the system is linear and homogeneous. In the next part we will analyze the dynamics of the plate including the effect of nonlinearities.

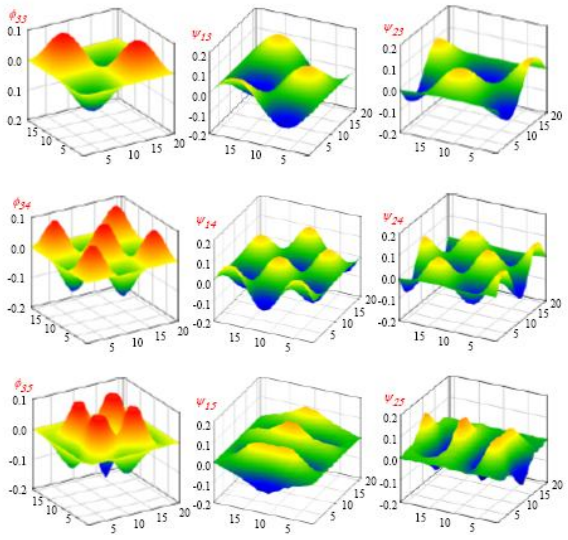


Fig.10: The third, fourth and fifth POD mode shapes.

CONCLUSIONS

There are similarities between the normal modes of vibrations and the POD modes obtained by processing the discrete free dynamics.

The POD modes provides direct measure of the coupled dynamics through the norms of the POD mode shapes.

This methodology can be expanded to analyze nonlinear dynamics aiming at obtaining optimum modes that may represent nonlinear normal of vibrations.

ACKNOWLEDGMENTS

Author would like to acknowledge the Applied Science private University for their support.

REFERENCES

[1] Berger H.M. 1955: A new approach to the analysis of large deflections of plates, Journal of Applied Mechanics. 22, 465-472.

[2] Georgiou, I. T., Bani-Khaled, M. A., 2003: Extracting Signatures for the Rigid Body Motion and Modes of Coupled Vibration in Elastic Multi-body Mechanisms by POD of the Finite Element Dynamics, ASME 2003 Design Engineering Technical Conferences and Computers and Information in Engineering Conference, Chicago, Illinois USA, September 2-6, 2003.

[3] Georgiou, I. T., Bani-Khaled, M. A., 2004: Identifying the shapes of coupled vibrations and deriving reduced order models for nonlinear shafts: a Finite Element-Proper Orthogonal Decomposition Approach. ASME International Mechanical Engineering Congress & Exposition Anaheim, California.

[4] Georgiou, I. T., Bani-Khaled, M. A., Bajaj, A., 2006: On the fundamental nature of geometric singular perturbations to characterize the interaction dynamics in flexible multi-body structural systems , 2nd International Conference on Nonlinear Normal Modes and Localization in Vibrating Systems, June 19-23, Karlovasi, Samos, Greece.

[5] Georgiou, I. T., Corless, M., Bajaj, A., 1999: Dynamics of Nonlinear Structures with Multiple Equilibrium States: a Singular Perturbation-Invariant Manifold Approach, ZAMP Journal of Applied Mathematics and Physics, Vol. 50, pp. 892-924.

[6] Georgiou, I. T., Schwartz, I. B., 2001: Invariant Manifolds, Non-classical Normal Modes, and Proper Orthogonal Modes in the Dynamics of the Flexible Spherical Pendulum, Nonlinear Dynamics, 25 (1-3), pp. 3-31.

[7] Haterbouch, M., Benamar, R., 2003: The effects of large vibration amplitudes on the axisymmetric mode shapes and natural frequencies of clamped thin isotropic circular plates, part I: iterative and explicit analytical solution for non-linear transverse vibrations. Journal of Sound and Vibration, 265, 123-154.

[8] Huang, C., L., Al-Khatta, I., M., 1977: Finite amplitude vibrations of a circular plate. International Journal of Non-Linear Mechanics. 12, 297-306.

[9] Kreuzer, E. 1987: Numerical Study of Non-Linear Dynamic. Berlin: Springer Press.

[10] Rao, G., V., Raju, K., K., 1980: Large amplitude axisymmetric vibrations of orthotropic circular plates elastically restrained against rotation. Journal of Sound and Vibration, 69, 175-180.

[11] Rao, G., V., Raju, K., K., Raju I., S., 1976: Finite element formulation for the large amplitude free vibrations of beams and orthotropic circular plates. Journal Computers and Structures. 6,169-172.

[12] Sathyamoorthy, M., 1988: Literature review: Recent research in nonlinear plate vibrations. The Shock and Vibration Digest. 20, 14-20.

[13] 13. Sathyamoorthy, M., Prasad, M. E., 1984: A multiple-mode approach to large-amplitude vibration of moderately thick elliptical plates. J. Appl. Mech. 51, 153-158.